Taylor & Francis
Taylor & Francis Group

Xenobiotica
the fate of foreign compounds in biological systems

ISSN: 0049-8254 (Print) 1366-5928 (Online) Journal homepage: http://www.tandfonline.com/loi/ixen20

New insights in the metabolism of Oxybutynin: evidence of N-oxidation of propargylamine moiety and rearrangement to enaminoketone.

Silvio Aprile, Rossana Canavesi, Rosanna Matucci, Cristina Bellucci, Erika Del Grosso & Giorgio Grosa

To cite this article: Silvio Aprile, Rossana Canavesi, Rosanna Matucci, Cristina Bellucci, Erika Del Grosso & Giorgio Grosa (2017): New insights in the metabolism of Oxybutynin: evidence of N-oxidation of propargylamine moiety and rearrangement to enaminoketone., Xenobiotica, DOI: 10.1080/00498254.2017.1342288

To link to this article: http://dx.doi.org/10.1080/00498254.2017.1342288

Accepted author version posted online: 13 Jun 2017.

New insights in the metabolism of Oxybutynin: evidence of *N*-oxidation of propargylamine moiety and rearrangement to enaminoketone.

Silvio Aprile[1*], Rossana Canavesi[1], Rosanna Matucci[2], Cristina Bellucci[2], Erika Del Grosso[1], and Giorgio Grosa[1]

[1]Department of Pharmaceutical Sciences – Laboratory of pharmaceutical analysis, University of Eastern Piedmont, L.go Donegani 2, 28100 Novara, Italy. [2]Department of Neuroscience, Psychology, Drug Research and Child's Health, University of Florence, V.le G. Pieraccini 6, 50139 Firenze, Italy.

[*]**Corresponding author:** Dr. Silvio Aprile; Department of Pharmaceutical Sciences – Laboratory of pharmaceutical analysis, University of Eastern Piedmont. L.go Donegani 2, 28100 Novara, Italy. tel +39 (0)321 375855, Fax 39 (0)321 375621, e-mail: silvio.aprile@uniupo.it

ORCID:

Silvio Aprile: 0000-0003-4804-9543

Rosanna Matucci: 0000-0003-1965-9748

Cristina Bellucci: 0000-0001-6968-6176

Erika Del Grosso: 0000-0002-2398-5944

Giorgio Grosa: 0000-0002-1562-556X

KEYWORDS

Oxybutynin; *N*-oxidation; *in vitro-in vivo* metabolism; mass spectrometry

ABSTRACT

1. Oxybutynin hydrochloride is an antimuscarinic agent prescribed to patients with an overactive bladder and symptoms of urinary urge incontinence. Oxybutynin undergoes pre-systemic metabolism, and the *N*-desethyloxybutynin (Oxy-DE), is reported to have similar anticholinergic effects.

2. We revisited the oxidative metabolic fate of oxybutynin by liquid chromatography tandem mass spectrometry analysis of incubations with rat and human liver fractions, and by measuring plasma and urine samples collected after oral administration of oxybutynin in rats. This investigation highlighted that not only *N*-deethylation, but also *N*-oxidation participates in the clearance of oxybutynin after oral administration.

3. A new metabolic scheme for oxybutynin was delineated, identifying three distinct oxidative metabolic pathways: *N*-deethylation (Oxy-DE) followed by the oxidation of the secondary amine function to form the hydroxylamine (Oxy-HA), *N*-oxidation (Oxy-NO) followed by rearrangement of the tertiary propargylamine *N*-oxide moiety (Oxy-EK), and hydroxylation on the cyclohexyl ring.

3. The functional activity of Oxy-EK was investigated on the muscarinic receptors (M_{1-3}) demonstrating its lack of antimuscarinic activity.

4. Despite the presence of the α,β-unsaturated function, Oxy-EK does not react with glutathione indicating that in the clearance of oxybutynin no reactive and potentially toxic metabolites were formed.

INTRODUCTION

Antimuscarinics are the mainstay of pharmacological treatment of overactive bladder (OAB), a complex disorder defined by the presence of urinary urgency, usually associated with frequency and nocturia, with or without urinary urge incontinence. Oxybutynin hydrochloride (4-diethylamino) but-2-ynyl(*RS*)-2-cyclohexyl-2-hydroxy-2-phenyl-acetate hydrochloride, Oxy) is an antimuscarinic agent administered as a racemic mixture and is widely prescribed to OAB patients with symptoms of urge incontinence. However, its antimuscarinic activity resides predominantly on the (*R*)-enantiomer, which binds selectively to muscarinic M_1 and M_3 receptors in the detrusor muscle. Today, different types of oxybutynin formulations are available, including immediate and extended release tablets, oral solutions, syrup and a solution for intravesical administration.

Oxybutynin is absorbed from the gastrointestinal tract following oral administration, with a systemic bioavailability of less than 10% when compared to intravenous dosing due to extensive pre-systemic metabolism. The circulating primary metabolite, *N*-desethyloxybutynin (Oxy-DE), is present in plasma at concentrations approximately 4-10 times those of the parent compound, while having anticholinergic effect similar to oxybutynin (Douchamps,et al., 1988 and Hughes et al., 1992). In therapeutic use, Oxy-DE appears to contribute greatly to the treatment-limiting anticholinergic side effects associated with the oral administration of oxybutynin (Zobrist et al, 2001). Consequently, to mitigate the systemic adverse effects occurring during therapy, topical formulations, such as an adhesive patch, were employed exploiting oxybutynin *free base* as the drug substance (Shaw et al., 2007, Mizushima et al., 2007, and Staskin et al., 2010).

In the past few decades, the metabolic fate of oxybutynin and its effect on drug metabolizing enzymes have been investigated in rats (Akimoto et al., 1986), dog, and human after oral administration (Shinozaki et al., 1986). The authors reported the formation of a multitude of metabolites in dog and human urine and estimated that up to ~ 30% of the administered dose was excreted as metabolites in urine; they also observed the highest metabolic activity in rat liver. Four metabolic pathways were identified: *N*-deethylation, hydrolysis of ester, hydroxylation at 3' and 4'

positions on the cyclohexane ring and the conjugation of the corresponding metabolites. In the same year Akimoto et al., (1986) reported that, cyclohexylmandelic acid (CHMA) is the main metabolite in rat plasma after the oral administration of oxybutynin, while the glycine conjugate is the main metabolite in bile and urine. More recently, carboxylesterase 1 (hCE1) was identified as the major isozyme responsible for oxybutynin hydrolysis (Sato et al., 2012). In 1998, Yaïch and co-workers (Yaïch et al., 1998) demonstrated that the CYP3A4 subfamily is involved in the formation of the Oxy-DE metabolite. Finally, Lindeke et al. (1981) first reported *N*-oxidation of the tertiary propargylamine moiety in rat liver microsomes using deuterated substrate and GC-MS analysis. However, they were not able to directly reveal the presence of the *N*-oxide metabolite (Oxy-NO), but detected its degradation products promoted by high temperature GC-MS analysis. Indeed, they proposed the formation of propenal and Schiff base derivatives by Oxy-NO rearrangement.

To the best of our knowledge, no further study has addressed the oxidative metabolic fate of oxybutynin in the last thirty years. In our previous report (Canavesi et al., 2016), we elucidated the chemical degradation pathway of oxybutynin *free base* in oxidative conditions; disclosing the role of oxybutynin *N*-oxide in the formation of oxybutynin enaminoketone (Oxy-EK), the final degradation product whose structure and mechanism of formation we established. In this paper, we revisit the oxidative metabolic fate of oxybutynin in rat and human liver microsomes and *in vivo* in rats, providing evidence for metabolic *N*-oxidation followed by rearrangement to Oxy-EK. We also explored the possible muscarinic profile of Oxy-EK, with the hypothesis that Oxy-EK binds to muscarinic receptor subtypes being tested in Chinese hamster ovary (CHO) cells stably expressing $M_{1\text{-}3}$ receptors.

EXPERIMENTAL

Reagents and chemicals

Acrylonitrile, atropine sulfate salt monohydrate, 1-chloroethyl chloroformate, *m*-chloroperbenzoic acid (*m*CPBA), methanol – HPLC grade, triethylamine, and uridine 5'-diphosphoglucuronic acid trisodium salt (UDPGA), were purchased from Sigma-Aldrich (Milano, Italy) or Alfa Aesar (Lancashire, UK). Adenosine 3'-phosphate 5'-phosphosulfate lithium salt hydrate – 80% (PAPS) and reduced glutathione (GSH) were purchased from Merck (Milano, Italy). [^{3}H]*N*-methylscopolamine chloride specific activity range 2,590–3,200 GBq/mmol and UniFilter GF/C plates from Perkin-Elmer Life and Analytical Science, Monza, Milano, Italy. Water (HPLC grade) was obtained from Milli-Q reverse osmosis system (Millipore Co., Billerica MA, USA). Column chromatography was performed on silica gel 60 (230-400 mesh ASTM Merck). Thin layer chromatography (TLC) was carried out on plates with a layer thickness of 0.25 mm (silica gel 60 F254; Merck); when necessary, they were visualized after spraying with ninhydrin reagent. Oxybutynin (potency: 99.3%), was obtained as gift sample from Pharmafar S.r.l. (Torino, Italy). Oxybutynin *free base*, Oxy-NO, and Oxy-EK were prepared according to the procedures previously reported (Canavesi et al., 2016).

Instrumentation and chromatographic conditions

LC-UV analyses

A Shimadzu HPLC system (Shimadzu, Kyoto, Japan), consisting of two LC-10AD Vp module pumps, a SLC-10A Vp system controller, a SIL-10AD Vp autosampler and a DGU-14-A on-line degasser, was used for the analysis. All the chromatographic separations were performed on a Kinetex C18 XB 150 × 4.6 mm (5 μm d.p.) column as a stationary phase protected by a C18-Security Guard™ (Phenomenex, Torrance, CA). The SPD-M10Avp photodiode array detector was used to detect the analytes at 210 and 311 nm. LC Solution 1.24 software was used to process the chromatograms. Aliquots (20 μl) of the supernatants obtained from the incubations were injected

onto the HPLC system. The isocratic mobile phase (flow rate 1.4 ml/min) was composed of eluant A ammonium acetate buffer (20 mM, pH=5.7) and eluant B methanol, with the A:B ratio being 35:65 (*v/v*) (total run time: 15 min). The eluants were filtered through a 0.45 μm pore size PVDF membrane filter prior to use. All of the analyses were carried out at room temperature.

LC-MS^n analyses

A Thermo Finningan LCQ Deca XP plus system equipped with a quaternary pump, a Surveyor AS autosampler, a Surveyor photodiode array detector and a vacuum degasser was used for LC-MS analyses (Thermo Electron Corporation, Waltham, MA). All the chromatographic separations were performed on a Kinetex C18 50 × 2.10 mm (2.6 μm d.p.) column protected by a C18-Security Guard™ (Phenomenex, Torrance, CA) kept at a 35 °C. Aliquots (5 μl) of supernatants obtained from incubations were injected onto the system and eluted with a mobile phase (flow rate 0.2 ml/min) consisting of: A ammonium acetate buffer (10 mM, pH 5.7), and eluant B methanol. The following gradient elution was used: 0 to 9.5 min [A=55-20%, B=45-80%], 9.5 to 10 min [A=20-55%, B=80-45%], 10 to 15 min [A=55%, B=45%]. The eluants were filtered through a 0.45-μm pore size polyvinylidene difluoride membrane filter before use. The eluate was injected into the electrospray ion source (ESI) and MS spectra were acquired and processed using Xcalibur® software. The operating conditions of the ion trap mass spectrometer were as follows: *positive mode*, spray voltage, 5.00 kV; source current, 80 μA; capillary temperature, 300 °C; capillary voltage, 22.00 V; tube lens offset, 20.00 V; multipole 1 offset, -4.25 V; multipole 2 offset, -8.00 V; sheath gas flow (N_2), 35 Auxiliary Units. *Negative mode*: spray voltage, 3.30 kV; source current, 80 μA; capillary temperature, 300°C; capillary voltage, -34.00 V; tube lens offset, -35.00 V; multipole 1 offset, 6.25 V; multipole 2 offset, 10.50V; sheath gas flow (N_2), 50 Auxiliary Units. Data were acquired in full-scan and product ion scan modes (MS^n) using mass scan range *m/z* 105-700. The collision energy was optimized at 28-30%.

Spectroscopic analyses

^{1}H and ^{13}C experiments were performed at 298 K on a JEOL Eclipse ECP 300 FT MHz spectrometer (Jeol Ltd. Tokyo, Japan) operating at 7.05T. Chemical shifts are reported in part per million (ppm).

Synthesis of the reference compounds

Benzeneacetic acid, α-cyclohexyl-α-hydroxy-4-(ethylamino)-2-butyn-1-yl ester (Oxy-DE)

Oxybutynin *free base* (1.32 g, 3.70 mmol) was dissolved in freshly prepared anhydrous dichloromethane (30 ml) and 1-chloroethyl chloroformate (2.22 ml, 20.6 mmol) was added dropwise maintaining the reaction temperature at 0°C under magnetic stirring. The reaction mixture was further heated to reflux for 1.5 hours, and after cooling at room temperature, the solvent was evaporated and the crude residue re-dissolved in methanol (30 ml) and heated to reflux for an additional 1.5 hours. Evaporation of the organic solvent under reduced pressure gave a yellow oil which was analyzed by TLC (dichloromethane/methanol 95:5, visualized with ninhydrin) obtaining three spots: (unreacted oxybutynin: R_f =0.5 red spot, Oxy-DE: R_f =0.2 yellow spot, unknown product: R_f =0.1 purple spot). The residue was purified by column chromatography using dichloromethane/methanol 95:5 and then 9:1 as eluant to give Oxy-DE as pale yellow oil (295 mg, 0.90 mmol, 24% yield, HPLC purity at 210 nm 95.8%), (Supplemental material Fig. 1).

ESI-MS: *calculated for $C_{20}H_{27}NO_3$ mol.wt.=329.4; found m/z 330 $[M+H]^+$.*

Benzeneacetic acid, α-cyclohexyl-α-hydroxy-4-(ethylamino)-4-(hydroxy)- 2-butyn-1-yl ester (Oxy-HA)

Oxy-DE (350 mg, 1.06 mmol) was dissolved in 5 ml of methanol in the presence of a catalytic amount of triethylamine. A small amount of water was then added to the mixture without leading the solution to be opalescent. Acrylonitrile (105 mg, 2.0 mmol) was added dropwise and the mixture was stirred at room temperature for five hours. The solvent was then evaporated under

reduced pressure giving benzeneacetic acid, α-cyclohexyl-α-hydroxy-4-(ethylamino)-4-(cyanoethyl)-2-butyn-1-yl ester, as a yellow oil (~300 mg) which was used directly without further purification.

This crude intermediate (~300 mg, ~0.78mmol) was dissolved in few millilitres of freshly prepared anhydrous dichloromethane and *m*CPBA (270 mg, 1.29 mmol, dissolved in dichloromethane), was added dropwise maintaining the reaction at -78°C under nitrogen for 3 hours. The reaction was further stirred at 0°C for 2 hours. After cooling at room temperature, the reaction mixture was washed with 10% aqueous sodium carbonate solution. The organic layer was dried over anhydrous sodium sulfate, filtered and evaporated under reduced pressure giving a crude oil which was first purified by column chromatography (dichloromethane/methanol 98:2) and then by a second column (petroleum ether/2-propanol 9:1) to give Oxy-HA as a pale yellow oil (85 mg, 0.25 mmol, 32 % yield, 97.3% purity by HPLC assay), (Supplemental material Fig. 1).

ESI-MS: *calculated for $C_{20}H_{27}NO_4$ mol.wt.=345.4; found m/z 346 $[M+H]^+$.*

^{1}H-NMR *(300 MHz, $CDCl_3$) δ 7.64-7.30(m, 5H-aromatic), 4.80(d, J=13.4 Hz, O-CH_2-C≡), 4.75(d, J=13.4 Hz, O-CH_2-C≡), 3.59(s, ≡CH_2-N), 2.75(q, J=7.14 Hz, N-CH_2), 2.24-1.09 (m, CH_3 and 11H-cyclohexyl).*

Rat and human liver preparations

Male Wistar Han rat liver microsomes (RLM), (protein concentration: 20 mg/ml, total P450: 650 pmol/mg protein), human liver microsomes (HLM), (pooled mixed sex, fifty individual donors, protein concentration: 20 mg/ml, total P450: 360 pmol/mg protein), and human liver cytosol (HLC), (pooled mixed sex, fifty individual donors, protein concentration: 20 mg/ml, sulfotransferase: 0.63 nmol/mg protein) were purchased from Corning B.V. Life Sciences (Amsterdam, The Netherlands). All the incubations were performed using a horizontal DUBNOFF shaking thermostatic bath (Dese Lab Research, Padova, Italy) while protecting from light.

Phase I incubations with RLM and HLM

The standard incubation mixture (0.5 ml final volume), was carried out in a 50 mM tris[hydroxymethyl]aminomethane (TRIS)/HCl buffer (pH 7.4) containing 3.3 mM $MgCl_2$, 1.3 mM $NADPNa_2$, 3.3 mM glucose 6-phosphate, 0.4 Units/ml glucose 6-phosphate dehydrogenase, 5 µl of acetonitrile (1% of total volume), and oxybutynin (200 µM). After pre-equilibration of the mixture, an appropriate volume of RLM or HLM suspension was added to give a final protein concentration of 1.0 mg/ml. The mixture was shaken for 60 minutes at 37°C. Control incubations were carried out without the presence of NADPH-regenerating system or microsomes. Each incubation was stopped by the addition of 0.5 ml ice-cold acetonitrile, vortexed and centrifuged at 12,500 rpm for 10 min. The supernatants were analyzed by LC-UV and LC-MS analyses. Alternatively, when the chemical reactivity of the metabolites was studied, GSH (3mM) was added to the incubation mixture. When Oxy-HA and Oxy-EK were studied as substrates, the incubations followed the same procedure reported above.

Phase II incubation HLM or HLC

Glucuronide

The standard incubation mixture, constituted by 2 mM UDPGA cofactor, in a 50 mM TRIS/HCl buffer (pH 7.4), containing 5 µl of acetonitrile (1% of total volume), oxybutynin or Oxy-HA (200 µM) was brought to a final volume of 0.5 ml. After pre equilibration of the mixture at 37 °C, an appropriate volume of HLM suspension, previously activated by Brij 58 surfactant (0.5 mg/mg protein) in ice for 15 min, was added to give a final protein concentration of 1.0 mg/ml. The incubation mixture was shaken for 60 minutes at 37°C. Control incubations were carried out in the absence of HLM or UDPGA cofactor. The incubations were stopped by addition of 0.5 ml ice-cold acetonitrile, vortexed and centrifuged at 12,500 rpm for 10 min prior to LC-MS analyses of the supernatants.

Sulfate

The standard incubation mixture, constituted by 0.1 mM PAPS cofactor, in a 50 mM TRIS/HCl buffer (pH 7.4), containing 5 µl of acetonitrile (1% of total volume), and compound Oxy-HA, brought to a final volume of 0.5 ml. After pre-equilibration of the mixture at 37 °C, an appropriate volume of HLC suspension was added to give a final protein concentration of 1.5 mg/ml. The incubation mixture was shaken for 60 minutes at 37°C. Control incubation was carried out in the absence of PAPS. Each incubation was stopped by addition of 0.5 ml ice-cold acetonitrile, vortexed and centrifuged at 12,500 rpm for 5 min. The supernatants were analyzed by LC-MS.

In vivo rat metabolism

Animals

Male Sprague Dawley (8-9 weeks, 250-300 g) rats were purchased from Envigo S.r.l. (Bresso, Italy). Animal studies were performed in accordance with EU and institutional guidelines approved by the

Bioethics Committee for Animal Experimentation of the University of Eastern Piedmont, Italy (Prot. DB064.11 - 14th September 2016). The animals were housed with free access to food and water and fasted for 16 h before administration. All the rats were maintained under a 12 h cycle of light/dark artificial lighting at 21-25 °C.

Oxybutynin administration and sample collection

Oxybutynin hydrochloride (75 mg/Kg) was administered to rats (*n*=8) by oral gavage (1.5 ml), dissolving the dose in saline. Blood samples were collected *via* the tail vein in heparinized tubes 1 and 2 h following the administration anesthetizing the rats with isoflurane. Urine samples were collected over the periods 0-6, 6-24 h and kept cool by placing the containers in ice. Blood samples were immediately centrifuged to obtain the plasma samples. All samples were stored at -80 °C until the analysis.

Determination of oxybutynin metabolites in rat plasma and urine

Preparation of calibration standards

Stock solutions of oxybutynin, Oxy-DE, Oxy-EK, and Oxy-HA were prepared in methanol at 1 mg/ml concentration. Standard working solutions were freshly obtained by serial dilution of the stock solutions with methanol. The calibration standards were prepared by spiking appropriate aliquots of working solutions (5µl) into blank plasma or urine (45 µl) and diluting with 100 or 50 µl of ice-cold acetonitrile respectively. Calibrators were homogenized and centrifuged at 12,500 rpm for 10 min. Supernatants (10 µl) were injected into the LC-MS system. The calibration curves ($y = ax + b$), were constructed from the peak areas versus analyte concentration (over a range of 5-1000 µg/l) using the weighted ($1/x$) linear least-squares regression method. Precision and accuracy were determined by repeated analyses ($n = 3$) of the five calibrators used to construct the calibration curve for each analyte. Precision was expressed as percent coefficient of variation (%CV), whereas the accuracy was determined as the percent relative error (%RE) of the mean back calculated concentrations from the theoretical concentrations. The mean precision (%CV) for all the analytes was ≤ 20%, whereas the mean accuracy (%RE) were 11.1%, 18.1%, 4.1%, and 17.8% for Oxybutynin, Oxy-DE, Oxy-EK and Oxy-HA respectively.

Plasma and urine samples preparation

Aliquots of plasma and urine samples (50 µl) were diluted by adding respectively 100 or 50 µl of ice-cold acetonitrile. Samples were homogenized and centrifuged at 12,500 rpm for 10 min. Supernatants (10 µl) were injected into the LC-MS system.

In vitro pharmacological characterization of Oxy-EK in human muscarinic receptor subtypes: displacement of [^{3}H]-N-methylscopolamine

^{3}H-NMS competition binding assays were carried out in polypropylene 96-well plates, using membranes from (CHO) cells stably expressing recombinant human M_1-M_3 muscarinic

acetylcholine receptors (mACh) receptors as previously described (Matucci et al., 2016). In general, membrane homogenates (30-70 μg/ml, final concentration) were incubated in 0.25 ml total volume of assay buffer (25 mM sodium phosphate containing 5 mM $MgCl_2$ at pH 7.4) containing [^{3}H]-NMS (0.2 nM) and a range of concentrations of oxybutynin and Oxy-EK at room temperature for 120 min; nonspecific binding was determined in the presence of 1 μM atropine. Receptor bound radioactivity was separated by filtration using UniFilter GF/C plates and was measured by scintillation counting. Results are expressed as means ± SEM of the percentage of inhibition (I%) of specific binding at 10 μM concentrations.

RESULTS

In vitro metabolism study

Phase I incubations with RLM and HLM

The *in vitro* metabolic fate of oxybutynin was assessed through its incubation in rat and human liver subcellular preparations in the presence or absence of a NADPH-regenerating system. The incubation samples were analyzed by both LC-UV and LC-MS to obtain data on the metabolic stability and the structures of the metabolites respectively. When the microsomal mixed-function oxidase system was activated by the presence of NADPH, oxybutynin underwent a relevant oxidative transformation with the residual substrate ranging from 10% (RLM) to 56% (HLM) (Supplemental material Fig. 2, 3). Similar values were obtained in incubations supplied with 3mM GSH with the residual substrate ranging from 15% (RLM) to 62% (HLM).

Structural characterization of oxybutynin metabolites was achieved by LC-MS tandem mass spectrometry analysis of the incubations carried out with HLM. All the metabolites were characterized based on their predicted mass shift from the oxybutynin protonated molecule at *m/z* 358, and the interpretation of their MS^n spectra. Oxybutynin incubation samples were analyzed in both positive full scan and product ion scan modes, revealing the phase I metabolites pattern reported in the chromatograms in Fig.1. As a matter of fact, the presence of eleven metabolite-

related ions was observed, whose MS^2 spectra and proposed fragmentation pathways are depicted in Fig. 2 and 3. Monitoring the ion at *m/z* 374, LC-MS^2 chromatogram revealed the presence of six peaks corresponding to the following metabolites: M1-M3 eluting at 3.37, 3.84, and 5.10 min respectively, Oxy-NO (7.15 min), Oxy-EK (9.52 min), and a minor metabolite M7 eluting at 4.60 min (Fig. 1).

Metabolites M1, M2, and M3 showed identical product ion spectra; among them, the MS^2 spectrum of M1 is reported in Fig. 3. For these metabolites, the protonated molecule at *m/z* 374 gave rise to a fragmentation pathway similar to that observed for oxybutynin. Indeed, the fragment ions at *m/z* 124, 142, and 258 correspond to those observed in the oxybutynin spectrum, whereas the fragments at *m/z* 187, 283 and 356 presented a shift of 16 Da with respect to the same ions found in the oxybutynin spectrum. Overall, this set of data suggested that the M1, M2, and M3 metabolites arose from enzymatic oxidation on the cyclohexane ring.

Oxy-NO product ion spectrum (*m/z* 374) gave two diagnostic fragment ions at *m/z* 189 and 171, corresponding to the same ions observed in the oxybutynin MS^2 spectrum (Fig. 3). Moreover, the presence of the fragment ions at *m/z* 356 (loss of water), and 158 (ester cleavage), both shifted by 16 Da with respect to the same ions in the oxybutynin spectrum clearly demonstrated that the enzymatic oxidation occurred on the propargylamine moiety, leading to the formation of *N*-oxide metabolite.

The structure of Oxy-NO was unequivocally confirmed by comparing its mass spectrum with that of synthetic Oxy-NO provided from the oxidation of oxybutynin *free base* with hydrogen peroxide (Canavesi et al., 2016).

Oxy-EK protonated molecules (*m/z* 374) generated a two-fragment MS^2 spectrum (Fig. 2). The most abundant ion (*m/z* 356) was due to the neutral loss of water whereas the ion at *m/z* 158 (generated from the ester cleavage) corresponded to the oxybutynin fragment ion at *m/z* 142 shifted by 16 Da. Considered together, these data indicated that the structure of Oxy-EK is identical to that of the degradation product previously reported in the chemical stability study of oxybutynin

(Canavesi et al.,2016). Even if the structure of Oxy-EK presents a potentially electrophilic *α,β*-unsaturated ketone function, its formation was not affected by the addition of GSH to the incubation, indicating the stability of the enaminoketone moiety.

The product ion spectrum of the minor metabolite M7 (*m/z* 374) gave similar fragmentation pathways to that of Oxy-NO (Supplemental material Fig. 4). The presence of the ions at *m/z* 158 (shifted of 16 Da respect to the same ion at *m/z* 142 in oxybutynin spectrum), and *m/z* 189 clearly indicated that the addition of an oxygen atom occurred on the *N*,*N*-diethyl propargylamino moiety. However, these data are insufficient to propose a structure for this metabolite.

The relevant literature currently states that Oxy-DE is the circulating primary metabolite after oxybutynin oral administration. It is characterized by a protonated molecule at *m/z* 330 whose fragmentation generated the ions at *m/z* 312 (loss of water) and *m/z* 230 (100 Da neutral fragment loss) which corresponded to the ion at *m/z* 258 observed in the oxybutynin spectrum. In liver microsomes, Oxy-DE underwent further oxidative *N*-deethylation generating the primary amine metabolite M6. The structure assignment was based on the presence of the protonated molecule at *m/z* 302, whose fragmentation generated the ions at *m/z* 284 (loss of water) and at *m/z* 202 (100 Da neutral fragment) which corresponded to the ion at *m/z* 230 observed in the Oxy-DE spectrum. Moreover, Oxy-DE underwent hydroxylation at the cyclohexane ring (metabolites M4 and M5) and *N*-oxidation generating the corresponding hydroxylamine Oxy-HA. In particular, metabolites M4 and M5 gave identical MS^2 spectra, as featured by the presence of the diagnostic ions at *m/z* 187, 215, and 283 (the same ions were found in the M1 spectrum), and the ion at *m/z* 230, resulting in the neutral loss of a 116 Da fragment. This fragmentation pattern indicated that the metabolites M4 and M5 arose from aliphatic hydroxylation on the cyclohexane ring. The secondary metabolite Oxy-HA gave a protonated molecule at *m/z* 346; the presence of fragment ions at *m/z* 171, 229 and 246 (loss of a 100 Da neutral fragment) indicated that oxidation on the propargylamine moiety had occurred. The structure of Oxy-HA was unequivocally confirmed by comparison of its retention time and fragmentation pathways with those of a synthetic standard. The formation of Oxy-HA was

observed when synthetic Oxy-DE was incubated in the same conditions as oxybutynin, confirming that it arises from the oxidation of secondary amino group. Finally, according to the results of Sato et al. (2012), the formation of the CHMA metabolite arising from the hydrolysis of ester function was observed in this study, confirming the presence of the ion at *m/z* 233 $[M-H]^-$ (data not shown).

Phase II incubations.

Glucuronidation and sulfation.

In order to assess the formation of glucuronide metabolites, HLM incubations of oxybutynin and Oxy-HA were carried out in the presence of UDPGA cofactor. The formation of sulfates was evaluated by incubating the same substrates in the presence of HLC fractions and the PAPS cofactor. All of the incubations were analyzed by LC-MS in negative ionization mode.

The formation of a metabolite eluting at 4.04 min was observed in the Oxy-HA incubation in the presence of UDPGA, while the same peak is absent in control incubations. The metabolite generated a deprotonated molecule at *m/z* 520, corresponding to the addition of 175 Da with respect to the parent compound, suggesting the formation of an Oxy-HA glucuronide (Fig.4). This attribution was further supported by the presence of the diagnostic fragment ion at 344 *m/z* (neutral loss of glucuronic acid) as well as the presence of additional fragments at *m/z* 502, 304 and 233 *m/z*. However, the formation of Oxy-HA glucuronide was not observed in oxybutynin incubation. Similarly, the formation of oxybutynin glucuronide was not observed due to the lack of the corresponding ion at *m/z* 532 (data not shown). Finally, in the incubation of Oxy-HA performed in HLC supplied by PAPS, the absence of peaks in the chromatogram monitoring the negative ion at *m/z* 424 indicated that sulfate metabolites were not formed (data not shown).

In vivo rat metabolism.

To assess the *in vivo* formation of the new metabolites Oxy-EK and Oxy-HA, a study was undertaken in rats. The analysis of plasma samples, collected 1 and 2 h following oxybutynin

administration, revealed the presence of the parent drug and its metabolites Oxy-DE, Oxy-EK, but the absence of Oxy-HA and its glucuronide (Supplemental Fig. 5-7). The same metabolites were observed in urine samples collected over the periods 0-6 h and 6-24 h. after the treatment (Supplemental Fig. 6-7). The availability of the synthetic reference compounds for Oxy-DE and Oxy-EK (Supplemental Fig. 8) allowed their quantification. In plasma samples, oxybutynin was detected at concentrations ranging from 34 to 431 µg/l, while both Oxy-DE and Oxy-EK were present in comparable amounts at a concentration lower than 10 µg/l. In the urine samples, the mean concentration of oxybutynin was lower with respect to plasma concentrations, while both Oxy-DE and Oxy-EK were present at concentrations up to 100 µg/l (Fig. 5).

Due to the intrinsic instability of Oxy-NO synthetic standard (Canavesi et al., 2016), only the qualitative evaluation of Oxy-NO metabolite was provided. As a result, a prominent peak related to the presence of Oxy-NO was revealed in both plasma and urine samples at each time point (Supplemental Fig. 9). The stability of Oxy-NO and its rearrangement to enaminoketone were also investigated in rat plasma and urine samples spiked with a freshly prepared solution of Oxy-NO (Supplemental Fig. 10A). Overall, the obtained stability profiles indicated the progressive conversion over time of Oxy-NO to Oxy-EK: the residual Oxy-NO ranges from 86%, when incubated in plasma for 2 h at 37°C, to 13%, when incubated in urine for 24 h at 37°C (Supplemental Fig. 10B). Interestingly, Oxy-NO resulted stabilized in spiked plasma and urine samples compared to the control incubations carried out in methanol. Finally, the relative amount of Oxy-NO and Oxy-EK resulted unchanged in the spiked samples stored at-80°C for 24h demonstrating the role of temperature in the Oxy-NO interconversion to Oxy-EK.

In vitro pharmacological characterization of Oxy-EK in human muscarinic receptor subtypes.

^{3}H-NMS competition binding assays, using membranes from CHO cells stably expressing the recombinant human M_1-M_3 mACh, revealed that Oxy-EK was devoid of significant affinity toward the receptors (Tab. 1).

DISCUSSION

Depending on their structural features, the metabolic stability of drugs could be strictly related to their chemical stability; hence, the integration of both aspects could be conveniently performed defining a unique chemical and metabolic stability space. Using this viewpoint, we re-investigated the metabolic fate of oxybutynin by exploiting the recent findings in its chemical stability, both *in vitro* (rat and human liver subcellular preparations) and *in vivo* in rats, focusing our attention on the oxidative transformation of the tertiary propargylamine amine moiety.

The results allowed us to delineate a new metabolic scheme for oxybutynin **(**Fig. 6), observing a certain regio-selectivity, with only the tertiary amine and the cyclohexyl moieties being oxidized. Three distinct oxidative metabolic pathways were observed, namely: *N*-deethylation (Oxy-DE and M6), *N*-oxidation (Oxy-NO and Oxy-HA), and the aliphatic hydroxylation on cyclohexane ring for both oxybutynin (M1-M3) and Oxy-DE (M4-M5). The *N*-oxidation of oxybutynin was previously proposed by Lindeke et al. (1981); however, due to the thermal instability of *N*-oxide, it could not be directly detected using high-temperature GC-MS analysis. In our study, we detected Oxy-NO by means of LC-MS^{n} analysis in rat and human liver microsomal incubations unequivocally assigning its structure by comparison of its spectral data with those of the authentic *N*-oxide generated by oxidation of oxybutynin with hydrogen peroxide. It is worth mentioning that Oxy-NO was found in a significant amount in urine, indicating that the rearrangement could not be so relevant in the context of the metabolic fate of oxybutynin in physiological conditions.

The presence of the unprecedented metabolite Oxy-EK was also observed, while its formation through the previously described intramolecular prototropic rearrangement of oxybutynin *N*-oxide, (Szabó and Hermecz, 2001, Canavesi et al., 2016), was proposed (Supplemental Fig. 11).

Another noteworthy aspect is the chemical and metabolic stability of Oxy-EK; no metabolite was generated from it when incubated as a substrate in rat and human liver microsomes. Despite the presence of an *α,β*-unsaturated keto-function, no chemical and enzyme-mediated reactivity (i.e. gluthatione *S*-transferases) with GSH was observed. These results corroborate with our previous data, where the presence of the *α,β*-unsaturated function on Oxy-EK does not give rise to genotoxic potential (Canavesi et al, 2016). These results are in agreement with our previous data dealing with the lack of genotoxicity of Oxy-EK as observed in Ames assay. These features could be explained by the lack of basicity of nitrogen in the enaminoketone moiety, and by the push-pull character of the central double bond that would impose a significant presence of a mesomeric and dipolar form. This would mitigate the Michael acceptor property of the *α,β*-unsaturated function.

Since Oxy-DE represents a primary metabolite found in significant amounts both *in vitro* and *in vivo* experiments, the *N*-oxidation of the secondary amine function to Oxy-HA and the *N*-deethylation to the primary amino metabolite M6, could be expected. Accordingly, the presence of the new metabolite Oxy-HA was observed in liver microsomal incubations and confirmed by means of the synthetic reference compound. Moreover, the formation of the corresponding glucuronide was also established after the incubation of Oxy-HA. Conversely, analysis of the plasma and urine samples excluded the presence of significant amounts of Oxy-HA and its glucuronide. This might not be surprising, considering that Oxy-HA was solely a minor *in vitro* metabolite of oxybutynin and the related glucuronide was only detected after Oxy-HA incubation with liver microsomes.

The literature shows that oxybutynin is well absorbed from the gastrointestinal tract following oral administration, but that its systemic bioavailability is less than 10% when compared to intravenous dosing due to extensive pre-systemic metabolism. The circulating primary metabolite, Oxy-DE, was found in plasma at concentrations approximately 4–10 times than those of the parent compound and

has similar anticholinergic effects to oxybutynin (Hughes et al., 1992, Zobrist et al., 2001). Based on our *in vivo* investigation, we demonstrated the presence of the parent drug and its metabolites Oxy-DE, Oxy-EK, and Oxy-NO in rat plasma and urine, following oral administration of Oxy. Taken together, both the *in vitro* and *in vivo* data demonstrated that Oxy-DE, Oxy-NO and Oxy-EK all participate in the clearance of oxybutynin after oral administration.

To assess the pharmacodynamics of the new metabolites, the activity of the chemically stable metabolite, Oxy-EK, on the three main muscarinic receptor subtypes ($hM_{1\text{-}3}$, widely expressed in peripheral systems), was investigated. The enaminoketone function of Oxy-EK could not be protonated at physiological pH (which differs from the propargylamine moiety of Oxy), mitigating its affinity with muscarinic cholinergic receptor, and accordingly, the experimental data showed that Oxy-EK is devoid of antimuscarinic activity.

In conclusion, taking together the *in vitro* and *in vivo* data, we highlighted that both the *N*-deethylation and *N*-oxidation metabolic pathways participate in the clearance of oxybutynin after oral administration. Moreover, we demonstrated the lack of antimuscarinic activity of the newly reported metabolite Oxy-EK, and the presence of the α,β-unsaturated function did not give rise to a genotoxic potential indicating that the clearance of oxybutynin does not produce an active or putatively toxic metabolite.

ACKNOWLEDGEMENTS

Financial support from the University of Eastern Piedmont, Novara, Italy, (MedChem-2015), is gratefully acknowledged.

DECLARATION OF INTEREST

The authors report no declarations of interest. The authors alone are responsible for the content and writing of this article.

REFERENCES

AkimotoY, Kobayashi H, Shinozaki Y, and Urakubo G. (1986). Studies on metabolic fate of oxybutynin hydrochloride (4). Metabolism in rat. Iyakuhin Kenkyu 17:1070-1077.

Canavesi R, Aprile S, Giovenzana GB, Di Sotto A, Di Giacomo S, Del Grosso E, and Grosa G. (2016). New insights in oxybutynin chemical stability: Identification in transdermal patches of a new impurity arising from oxybutynin *N*-oxide rearrangement. Eur J Pharm Sci 84:123-131.

Douchamps J, Derenne F, Stockis A, Gangji D, Juvent M, and Herchuelz A. (1988). The pharmacokinetics of oxybutynin in man. Eur J Clin Pharmacol 35:515-520.

Hughes KM, Lang JC, Lazare R, Gordon D, Stanton SL, Malone-Lee J, and Geraint M. (1992). Measurement of oxybutynin and its *N*-desethyl metabolite in plasma, and its application to pharmacokinetic studies in young, elderly and frail elderly volunteers. Xenobiotica 22:859-69.

Lindeke B, Hallström G, Johansson C, Ericsson O, Olsson LI, and Stromberg S. (1981). Metabolism of Oxybutynin: establishment of desethyloxybutynin and oxybutynin *N*-oxide formation in rat liver preparation using deuterium substitution and gas chromatographic mass spectrometric analysis. Biomed Mass Spectrom 8:506-513.

Matucci R, Nesi M, Martino MV, Bellucci C, Manetti D, Ciuti E, Mazzolari A, Dei S, Guandalini L, Teodori E, Vistoli G, Romanelli MN. (2016). Carbachol dimers as homobivalent modulators of muscarinic receptors. Biochem Pharmacol 108:90-101.

Mizushima H, Kinoshita K, Abe K, Ishizuka H, and Yamada Y. (2007). Pharmacokinetics/pharmacodynamics analysis of the relationship between the in vivo micturition pressure and receptor occupancy of (R)-oxybutynin and its metabolite in rats. Biol Pharm Bull 30:955-962.

Sato Y, Miyashita A, Iwatsubo T, and Usui T. (2012). Conclusive identification of the oxybutynin-hydrolyzing enzyme in human liver. Drug Metab Dispos 40:902-906.

Shaw GL, and Pate HR. (2007). Transdermal oxybutynin: a review. Expert Opin Drug Metab Toxicol 3:435-439.

Shinozaki Y, Monden R, Manaka A, Hisa H, Naito S, Igarashi T, Sakai H, Iwata Y, Kasama T, Akimoto Y, and Urakubo G. (1986). Studies on metabolic fate of oxybutynin hydrochloride (3). Metabolism in human and dog and the site of biotransfornation and the effect on enzymes induction in the rats. Drug Metab Pharmacokinet 1:341-352.

Staskin DR, and Salvatore S. (2010). Oxybutynin topical and transdermal formulations: an update. Drugs Today 46:417-425.

Yaïch M, Popon M, Medard Y, and Aigrain EJ. (1998). *In-vitro* cytochrome P450 dependent metabolism of oxybutynin to *N*-deethyloxybutynin in humans. Pharmacogenetics 8:449-451.

Szabó, A and Hermecz I. (2001). Novel intramolecular rearrangement of tertiary propargylamine *N*-oxides. J Org Chem 66:7219–7222.

Zobrist RH, Schmid B, Feick A, Quan D, and Sanders SW. (2001). Pharmacokinetics of the R- and S-enantiomers of oxybutynin and *N*-desethyloxybutynin following oral and transdermal administration of the racemate in healthy volunteers. Pharm Res 18:1029-3104.

FIGURE CAPTIONS

Figure 1. Positive LC-MS^2 chromatograms of oxybutynin incubation in HLM.

Figure 2. LC-MS^2 spectra and fragmentation pathways of oxybutynin and Oxy-DE, Oxy-HA, and Oxy-EK metabolites.

Figure 3. LC-MS^2 spectra and fragmentation pathways of M1, M4, M6, and Oxy-NO metabolites.

Figure 4. LC-MS^2 chromatogram and fragmentation pathways of Oxy-HA glucuronide metabolite.

Figure 5. Mean plasma and urine concentrations of oxybutynin, Oxy-DE, and Oxy-EK. Oral administration of oxybutynin hydrochloride in male rats at a dose of 75 mg/Kg (mean ± S.E.M., *n*=8).

Figure 6. Proposed *in vitro*, *in vivo* metabolic pathways of oxybutynin.

TABLES

Table 1. Experimental values of binding data for oxybutynin and Oxy-EK with different human mACh receptors subtypes.

	I%		
compound	hM_1	hM_2	hM_3
Oxy	99.19 ± 0.53	99.55 ± 0.45	99.90 ± 0.10
Oxy-EK	10.27 ± 0.66	6.15 ± 1.25	28.15 ± 4.35

Percentage of inhibition (I%) of specific binding at 10 μM concentration.Values are means ± S.E.M. from three separate determinations in duplicate.

FIGURE 1

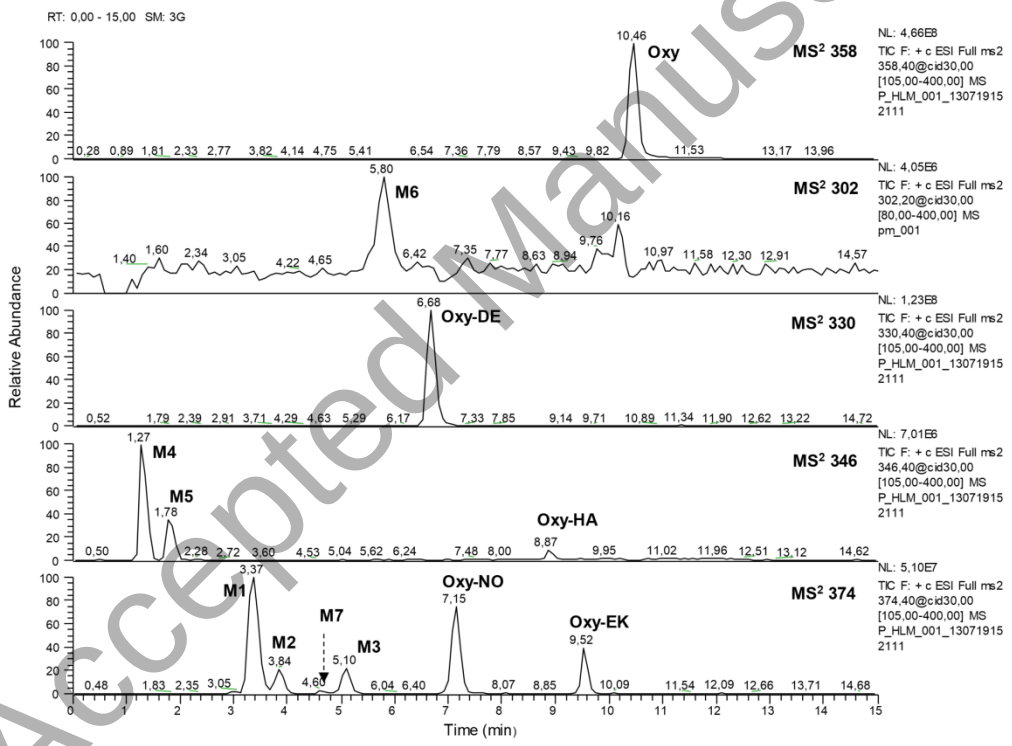

FIGURE 2

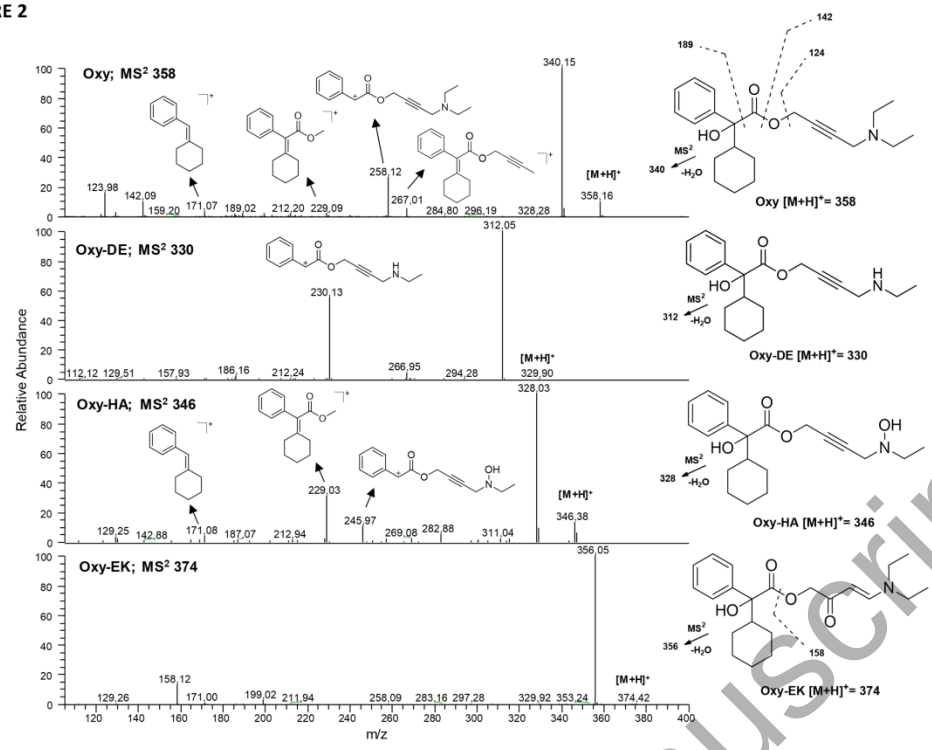

FIGURE 3

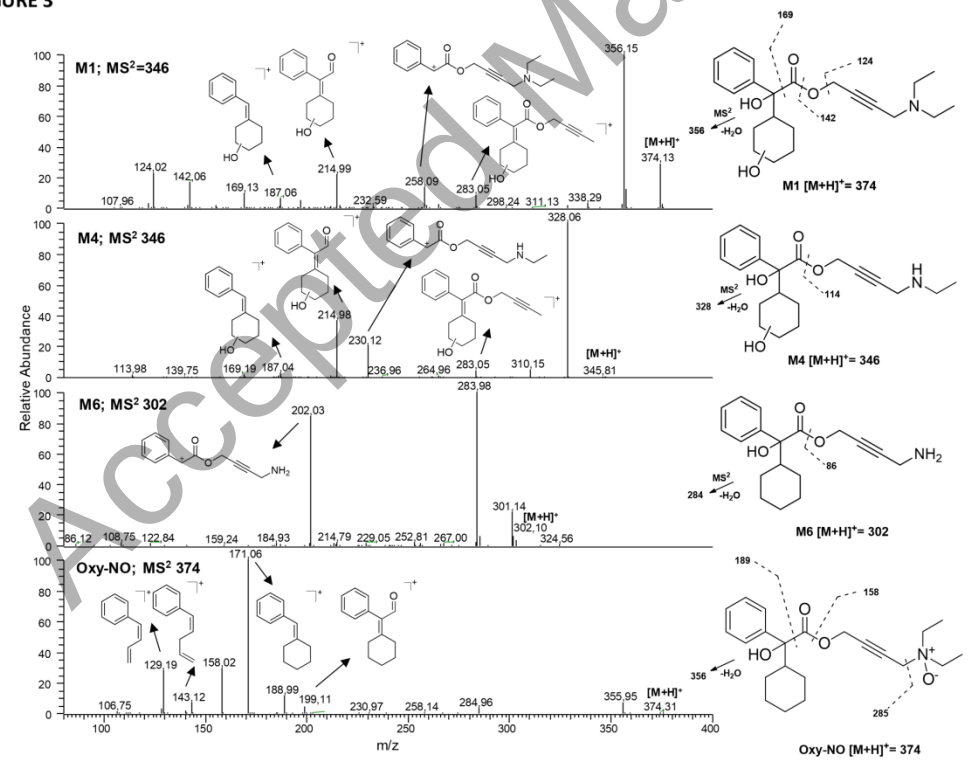

FIGURE 4

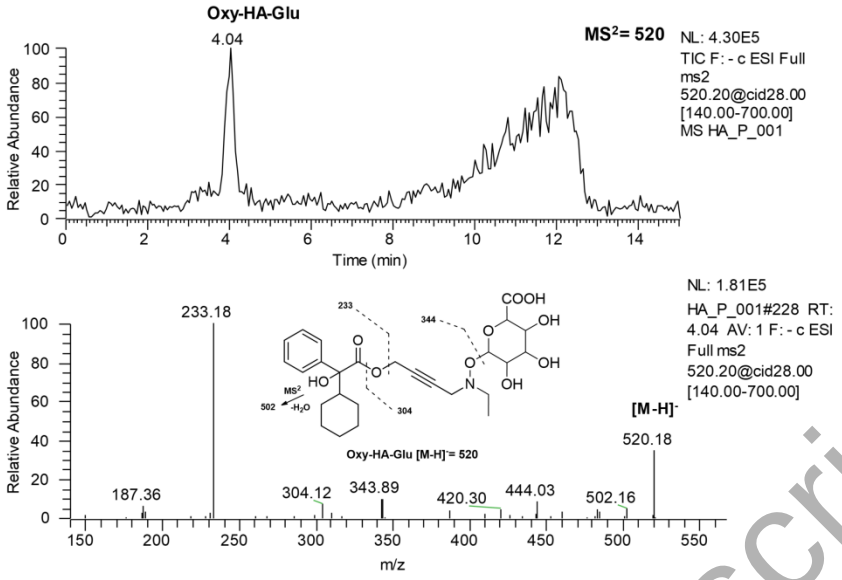

FIGURE 5

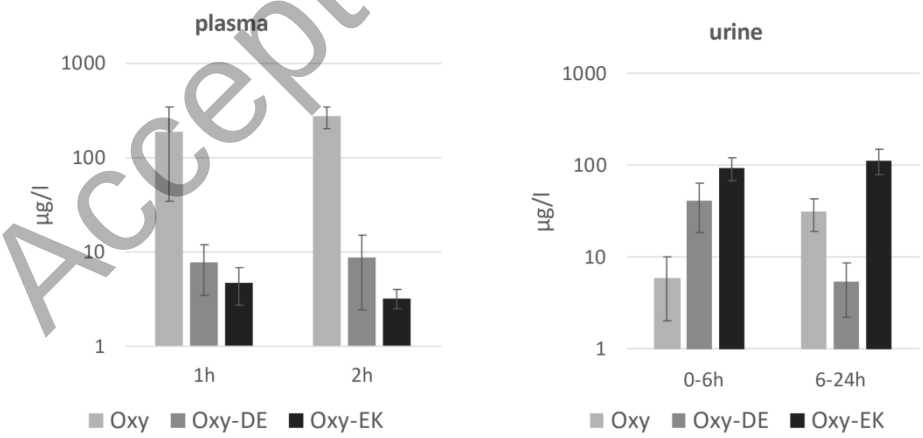

FIGURE 6